Journal of Applied Polymer Science

Ductile tear behavior of multilayered polypropylene homopolymer/ethylene 1-octene copolymer sheets

Guansong He,[1,2] Fengshun Zhang,[1,2] Huaning Yu,[1] Jiang Li,[1] Shaoyun Guo[1]

[1]The State Key Laboratory of Polymer Materials Engineering, Polymer Research Institute of Sichuan University, Chengdu 610065, China

[2]China Academy of Engineering Physics, Institute of Chemical Materials, Mianyang, Sichuan 621900, China

Correspondence to: J. Li (E-mail: li_jiang@scu.edu.cn)

ABSTRACT: The tear resistance of the polypropylene homopolymer (HPP)/ethylene 1-octene copolymer (POE) alternating multilayered sheets, which were prepared through multilayered coextrusion, was evaluated. Polarized optical microscope (POM) photographs revealed that HPP and POE layers aligned alternately vertical to the interfaces and continuously parallel to the extrusion direction. Tear results demonstrated the conventional blends had less tear-resistant than the multilayered samples. Large plastic deformation of HPP layer occurred in the multilayered structure during the stable crack growth, causing the tear energy to increase with the number of layers increasing. The measurements of PCMW2D IR and WAXD revealed that the large plastic deformation had a direct relationship with the crystal structure and termination of micro-cracks by interface. © 2016 Wiley Periodicals, Inc. J. Appl. Polym. Sci. **2016**, *133*, 43298.

KEYWORDS: mechanical properties; polyolefins; structure-property relations

Received 26 September 2015; accepted 1 December 2015

DOI: 10.1002/app.43298

INTRODUCTION

Resistance to tear is one of the important mechanical properties of flexible materials such as thin polymer sheets, etc.[1] Especially for the polyolefin packaging films, it will become a key property. Thermoplastic elastomers prepared by simple blending of a crystalline plastic and an elastomer have nowadays been used in many packaging applications due to their easy preparation and combined properties of thermoplastic and elastomer. However, most of the thermoplastic elastomer blends are found to be incompatible due to the poor interfacial interaction between the homopolymers. As a result, these incompatible blends exhibit poor tear properties.[2,3]

Recently, the morphology and mechanical properties of binary polymer blends have been extensively studied. It is found that the control of phase morphology is an effective route to increase the mechanical property.[4] The multilayered polymer blend could possess a better mechanical property compared with dispersed and cocontinuous blends, due to its best phase continuity in the direction of the acting force.[5–7] And the effect of poor interfacial interaction on the mechanical property in the multilayered structure could be weakened. Shen *et al.* found the yield strengths of multilayered blends were higher than those of conventional blends according to an equivalent box model.[8] Moreover, through the interaction between the crazing and shear-banding those were formed at the interface, the multilayered polycarbonate (PC) and styrene-acrylonitrile copolymer (SAN) materials could present ductile tensile fracture behavior.[9–11] And our previous studies showed that the fracture toughness of multilayered propylene–ethylene copolymer (CPP)/polypropylene homopolymer (HPP) was higher than that of conventional blends with the same components by essential work of fracture (EWF).[12] However, the tear behavior and the associated fracture mechanism of multilayered blends have received less attention due to the difficulty to obtain the alternating layered samples.

Wu *et al.* found that laminating through LLDPE with other polymeric films could result in an anti-synergistic effect, and the tear resistance became equal or less than that of LLDPE film alone.[13] However, in this study, the multi-layer film had only up to three layers, and the double sided adhesive tape was used as the binding layer. Thus it could not give an effective feedback to the research of tear resistance evaluation of multilayered sheets obtained by continuous on-line processing. More importantly, the effect of layer number on the tear resistance behavior couldn't be investigated through this method. In fact, the layer number and interface can have a dramatic effect on the mechanical properties of multilayered sheets. For example, with the number of layers increasing, more crazing and shear-banding interactions could formed at the interface, resulting that both the multilayered PC/SAN and PC/PMMA samples

exhibited much better ballistic performance than those with fewer layers.[14] And for the multilayered polymer sheets, the fracture toughness could increase with the layer number if the interfacial delamination occurred during the crack propagation.[15]

In addition, tear resistance can be strongly influenced by process conditions, which affect crystalline and amorphous orientation.[16] For the blown films of polyethylene and high melt strength polypropylene (hmsPP) blends, the crystalline morphology of PP could have an important effect on the tear behaviors. Balanced tear characteristics of polyethylene film were obtained by the nearly isotropic lamellar morphology, while the highly oriented shish-kebab morphology of hmsPP domains in the blend films resulted in an anisotropic tear behavior.[17] Moreover, the ductile tear characteristics of PP films were essentially achieved through the plastic deformation process, which largely depended on the crystalline nature of PP.[18,19]

In this work, the alternating multilayered HPP/POE sheets with 16 and 64 layers were prepared by multilayered coextrusion technology that was developed in our lab. For comparison, the neat HPP and conventional blend HPP/POE sheets were also extruded with an extruder of multilayered coextrusion system. Then, the effect of phase structure and layer number on the tear resistance of multilayered structure sheets can be investigated. At last, the tear tests of all samples were conducted using an ASTM standard Die C type tear test, which could measure the tear initiation and propagation.[20–22]

EXPERIMENTAL

Materials

The HPP used in this article was T38F from Lanzhou Petrochemical Company (China) with a melt flow rate (measured at 230 °C and 2.16 kg) of 3.0 g/10 min. The POE was Engage 8150 from Dupont-Dow Chemical consisting of 25 wt % octane, with a melt flow rate (measured at 190 °C and 2.16 kg) of 0.5 g/10 min.

Specimens Preparation

Multilayered sheets consisted of alternating HPP and POE layers were extruded using multilayered coextrusion system, as described previously.[8,23] The 16- and 64-layer specimens were extruded by varying the number of laminating-multiplying elements (LMEs). To ensure the consistency of POE content in the extrusion sheets, the screw speed ratio of two extruders was fixed. The temperature profile of extruders was in the range of 140–190 °C for HPP and POE. And the temperatures of LMEs and coextrusion block were both 190 °C. For comparison, the neat HPP and conventional blended HPP/POE specimens, which were first pelletized using a twin-screw extruder, were also extruded as sheets with the same dimension as the multilayered sheets using an extruder of multilayered coextruder system. The LMEs were not used for producing the neat HPP and conventional blended HPP/POE specimens.

Polarized Optical Microscope (POM)

POM (BX51, OLYMPUS, Japan) equipped with a video camera was used to observe the multilayered morphologies and tear fracture morphologies of composites. Before observation, an ~10-μm thin slice was obtained by a microtome along the extrusion direction.

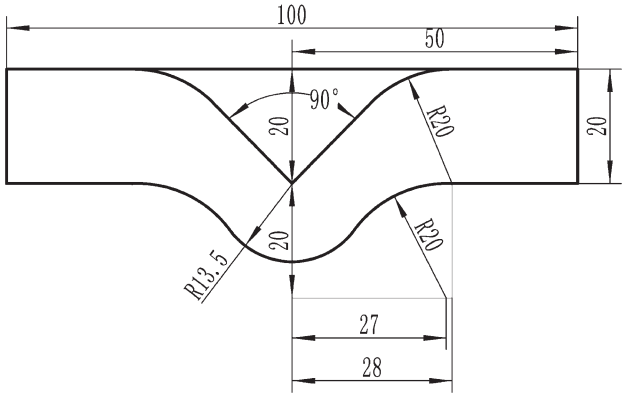

Figure 1. Profile and detailed dimensions (mm) of the Die C type tear specimen.

Tear Tests

The tear resistance of Die C type tear specimen, the profile of which is shown in Figure 1, was conducted on an Instron 5567 tension machine (Canton, MA) at a rate of 200 mm min^{-1} with an experimental temperature of 23 °C in accordance with ASTM D1004-90. The load–displacement curves were recorded. The tear strength can be calculated as follows:

$$T_S = \frac{F}{d} \quad (1)$$

where T_s is the tear resistance (KN m^{-1}), and F is the maximum force (N), and d is the specimen thickness (mm). At least of six specimens for each sample were tested and the average value was calculated. In addition, the energy that was absorbed until failure, expressed as tear energy, was calculated by the computer integration of the load-displacement curves. Compared with tear strength, the tear energy is more representative of the crack propagation resistance.[21]

FTIR Spectroscopy and 2D-IR Correlation Analysis

The time-resolved FTIR measurements were performed on a Nicolet iS10 FTIR instrument from Thermo Fisher Scientific. The thin sample film (15 μm) was placed in a homemade temperature control instrument including program heating cell. The temperature-dependent absorbance IR spectra in the 4000–400 cm^{-1} region were measured at a resolution of 4 cm^{-1}. The number of the scans of each spectrum was 20.

The film disk sample was heated from 25 to 205 C at a constant rate of 5 C min^{-1}.

And ~88 IR spectra were collected. The wavenumber regions were selected first and processed with a linear baseline correction. All the 2D-IR correlation spectra were calculated by two-dimensional correlation spectroscopy program designed in our laboratory based on MATLAB 7.0, as described in our previous study.[24] The contour images of the 2D correlation spectra were drawn through Origin Pro 8.0, and the filled red and blue area represented the positive and negative correlation intensity, respectively.

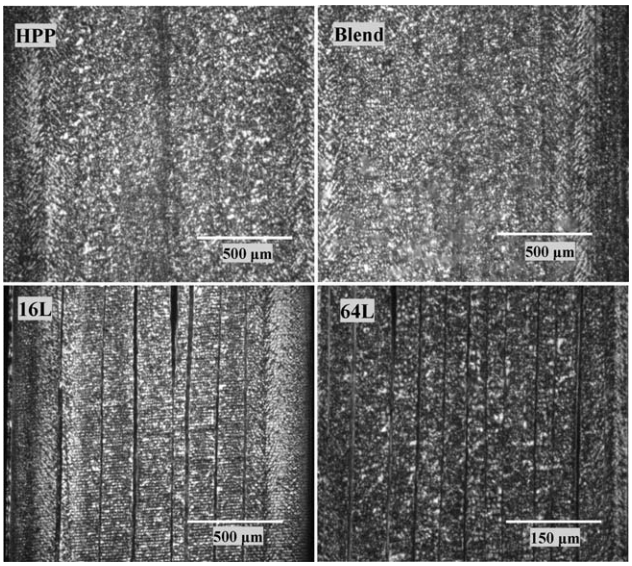

Figure 2. Polarized optical micrographs of the neat HPP, conventional blend and multilayered HPP/POE composites.

Wide-angle X-ray Diffraction (WAXD)

WAXD measurements were conducted on a DX-2500 X-ray Diffractometer (Dandong Fangyuan Instrument) with Cu Kα radiation ($\lambda = 1.5406$ Å) at a generator voltage of 40 kV and a current of 25 mA. The beam was filtered with a graphite monochromator. The samples were cut from the extruded polymer sheets. All experiments were carried out in the 2θ range of 5–35° at ambient temperature with a scanning speed of 0.03° s^{-1} and step size of 0.02°.

RESULTS AND DISCUSSION

Phase Morphology

Figure 2 shows the POM micrographs of the neat HPP, conventional blend and multilayered HPP/POE composites morphologies. For multilayered specimens, the darker and thinner layer belonged to the POE, which had a low crystallinity, while the whiter and thicker layer belonged to the HPP, which had a high crystallinity and exhibited a common spherulitic structure. It can be found that both the 16-layer and 64-layer specimens had a laminar morphology, where the HPP and POE layers were continuous and aligned alternately vertical to the interfaces. However, the conventional blend, which possessed the same volume fraction of POE as the multilayered specimens, had a morphology similar to "island phase" structure, where a small amount of POE was dispersed in the HPP matrix. And obviously the individual phase continuity along the extrusion direction became lower. In addition, through the measuring the thicknesses of the CPP and HPP layers in the POM micrographs, a method which was described detailed in our previous studies,[12] the volume fractions of the POE in the multilayered structure were found to have the same value of ~12%. As all of the multilayered sheets were prepared with the same processing conditions, including the same temperature and extruder speed, the proportions of two components did not change much with the number of layers.

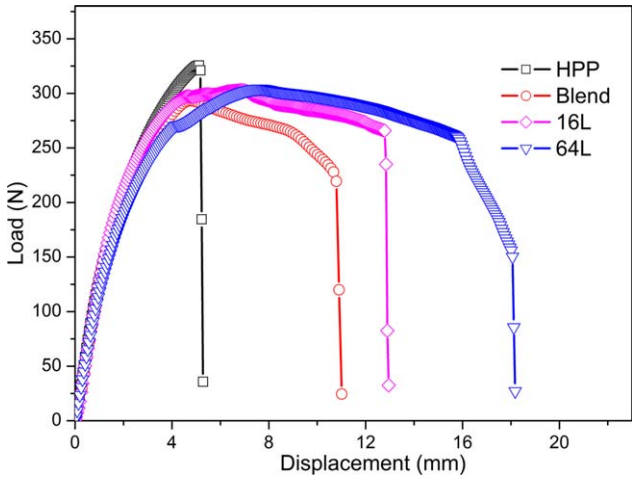

Figure 3. The tear load-displacement curves of HPP and HPP/POE specimens with a POE content of 12 vol %. [Color figure can be viewed in the online issue, which is available at wileyonlinelibrary.com.]

Tear Results and Fracture Morphologies

The typical load–displacement curves of HPP, multilayered, and conventional composites during tear testing are shown in Figure 3. For all samples, the load increased quickly with the increase of the displacement before the maximum load point. Then, the sample began to yield and the initiated cracks propagated until the final fracture. The HPP was tore with a highest load and a smallest displacement, revealing a characteristic of brittle fracture behavior. With the addition of elastomer POE, the tear loads of both conventional blend and multilayered specimens decreased, indicating the tear strength decreased. However, the final tear fracture displacement increased. Moreover, it was found that the final fracture displacement of multilayered specimens was larger than that of conventional blend specimen, and could increase with the number of layers increasing. The 64-layer specimen had a largest tear displacement.

The tear strength and energy obtained from the load-displacement curves are shown in Figure 4. It was found that the neat HPP obviously had a highest tear strength and a lowest tear energy. After the addition of elastomer POE, the tear

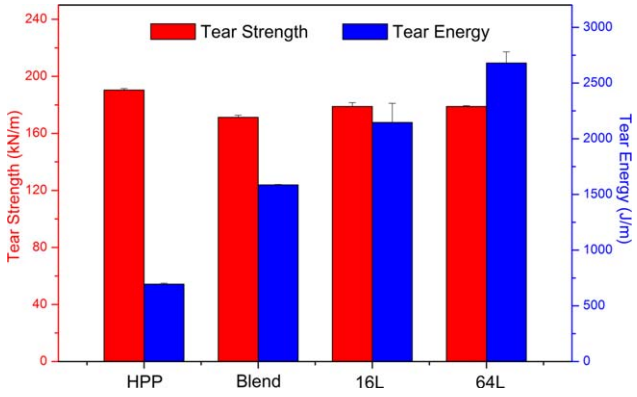

Figure 4. The tear strength and energy of HPP/POE specimens. [Color figure can be viewed in the online issue, which is available at wileyonlinelibrary.com.]

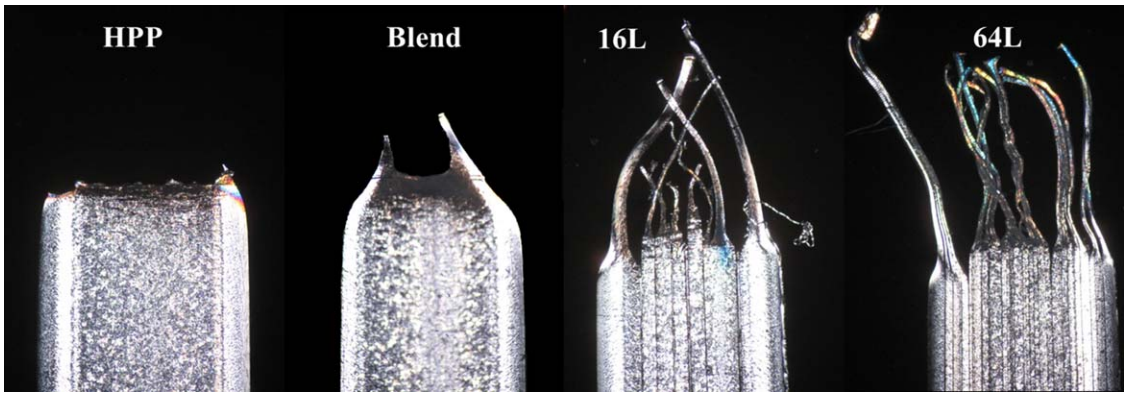

Figure 5. The POM images of HPP and HPP/POE slices of the fracture samples, and the arrow indicates the direction of melt flow. [Color figure can be viewed in the online issue, which is available at wileyonlinelibrary.com.]

strength decreased slightly but the tear energy increased greatly. As the addition of elastomer POE could improve the toughness of the PP/POE blends and decrease their stiffness.[25] The tear strengths of multilayered samples were a little higher than that of blend sample due to the best phase continuity of multilayered structure in the direction of the acting force.[3] More importantly, it was worth noting that the tear energies of 16-layer and 64-layer samples were obviously higher than that of conventional blend sample, and the tear energy of multilayered samples could increase with the number of layers. The 64-layer sample had the highest tear energy, i.e. the crack propagation resistance.

To compare the extent of fracture surface roughness for different HPP/POE specimens, the thin profile slice, which was perpendicular to the tear fracture surface, was obtained by a microtome along the direction of melt flow, and then observed with POM. The obtained images are shown in Figure 5. It was found that the deformation of neat HPP was very small, implying a brittle tear behavior. With the addition of POE, the conventional blend sample could produce some plastic deformation during tearing process. And for the 16-layer and 64-layer samples, the more significant plastic deformation behaviors could be found at the HPP layers. In particular, the degree of plastic deformation of HPP layers increased with the number of layers increasing. And the largest deformation of HPP occurred in the 64-layer sample. As a matter of fact, the plastic deformation behavior of HPP was contributed to energy absorption during tearing process, and was responsible for the high tear energy.

The PCMW2D Correlation Analysis

As stated above, the high tear energy was directly related to the mechanical plastic deformation of HPP, the latter of which was determined by the microstructure. As a semicrystalline polymer, the change of microstructure, mainly including the crystal form, crystallinity, and crystal size, can remarkably influence the mechanical deformation properties of polypropylene.[26,27] Therefore, it is necessary to study the crystallization properties of HPP in the HPP/POE systems. In recent years, the Fourier transform infrared spectroscopy (FTIR), a powerful method that is sensitive to chain conformations of crystalline region and amorphous region, has been applied to study the molecular structure and conformational adjustments of semicrystalline polymers.[28] However, the data obtained by the traditional FTIR analytical methods was static, and could result in the loss of some significant information on conformational changes during the melting and crystallization processes of polymers. To solve this problem, a new two-dimensional correlation method called perturbation correlation moving-window two-dimensional (PCMW2D) correlation spectroscopy was proposed by Morita,[29] and have been successfully applied to investigate the structural changes of PP during melting and crystallization processes. In this work, PCMW2D correlation spectroscopy technology was adopted to understand conformational changes of crystalline and amorphous region during the melting processes of PP. Then more information about the crystal structure of PP would be found.

Figure 6 shows the calculated PCMW2D correlation spectrum of HPP (25–205 °C) in the region 1201–1120 cm^{-1} for HPP and all HPP/POE systems. The band at 1166 cm^{-1} is assigned to the C—H rocking vibration of —CH_3 in the crystalline phase, while the band at 1153 cm^{-1} is assigned to the C—H rocking vibration of —CH_3 in the amorphous phase. With the increase of temperature, the peak at 1166 cm^{-1} would disappear while the peak at 1153 cm^{-1} would arise, revealing the melting process of the crystalline phase of polypropylene. For the neat HPP, at ~65 °C, there was a weak correlation peak at 1166 cm^{-1}. This belonged to the melting of some imperfect crystals in the crystalline phase. At ~159 °C, there was a strong correlation peak at 1166 cm^{-1} in Figure 6(a). And this belonged to the melting of the crystalline phase, i.e. the melt point of polypropylene. In addition, a tail-like part existed at the major crystalline peak at 1166 cm^{-1}, indicating some unstable crystals, such as β crystal, existed in the extruded HPP sheets. These unstable crystals began to melt at the low temperature. However, for the conventional blend sample displayed in Figure 6(b), there was no tail-like part at the major crystalline peak, and the melt point of some imperfect crystals in the crystalline phase became higher. That is to say there was no unstable crystal in the blend sample. For the multilayered samples displayed in Figure 6(c,d), the melt points of some imperfect crystals in the crystalline phase became more lower compared with that of the neat HPP. It means that the crystals became more imperfect in the multilayered structure. And the tail-like part of the major crystalline peak also became longer. This might indicate that more unstable

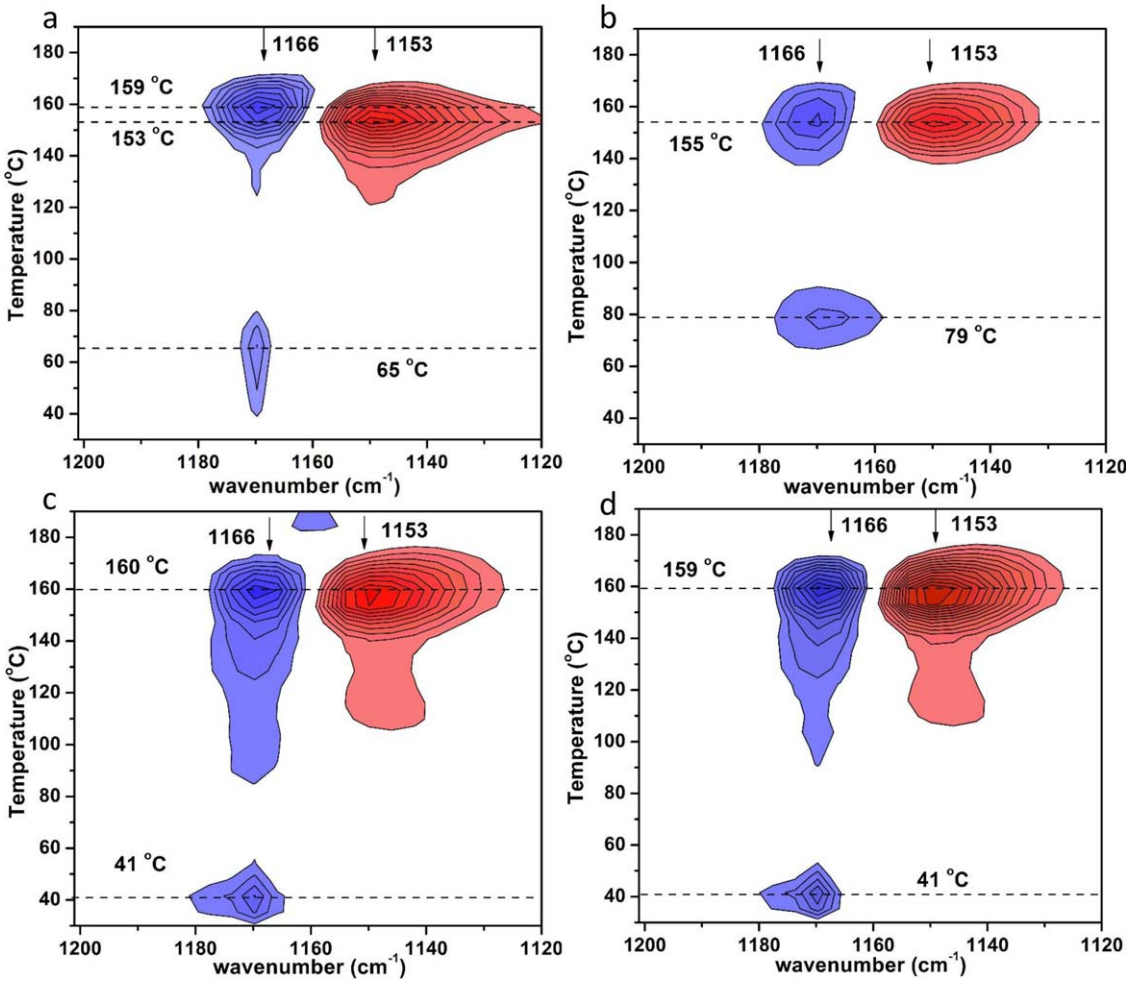

Figure 6. The PCMW2D correlation spectrum based on auto-correlation calculated from the temperature-dependent IR spectra of HPP (25–205 °C) in the region 1201–1120 cm^{-1} for: (a) the neat HPP; (b) the blend sample; (c) the 16-layer sample; (d) the 64-layer sample. [Color figure can be viewed in the online issue, which is available at wileyonlinelibrary.com.]

crystals existed in the multilayered HPP/POE sheets. Obviously, these unstable crystals and conformational changes of crystalline and amorphous region, which were found through PCMW2D correlation spectroscopy, could have a relationship with the mechanical properties of PP. Next, the crystal form and the content of unstable crystals should be further confirmed by WXRD.

Crystal Structure of HPP Determined by WAXD

The WXRD patterns of pure HPP, multilayered and conventional HPP/POE blends are given in Figure 7. The peaks at 14.01, 16.78, 18.42, 21.09, and 21.76° correspond to [110], [040], [130], [111], and [041] diffractions of α form crystals with a monoclinic configuration, respectively. The peak at 16.03° is the characteristic [300] diffraction of the β form crystals with a hexagonal configuration.[30] From Figure 7, it was found that α form and β form of PP crystals coexisted in the HPP, 16-layer and 64-layer samples. And there were no unstable β form PP crystals in the blend sample. This was consistent with the results of PCMW2D.

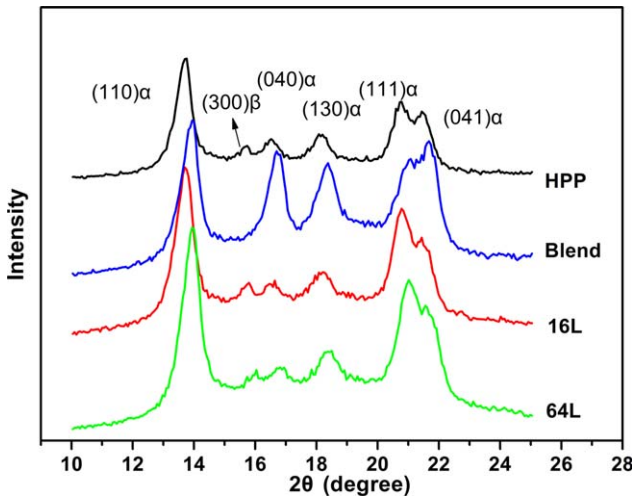

Figure 7. WXRD curves of HPP, multilayered and conventional PP/POE blends. [Color figure can be viewed in the online issue, which is available at wileyonlinelibrary.com.]

Table I. WXRD Data of HPP, Multilayered, and Conventional Blends

Sample	Diffraction peak	2θ/°	d/Å	β/°	L_{hkl}/Å	k	X_c
HPP	(110) α	13.70	6.46	0.51	157	9.69%	46.49%
	(300) β	15.69	5.64	0.49	164		
	(040) α	16.52	5.36	0.68	118		
	(130) α	18.14	4.88	0.71	113		
Blend	(110) α	13.91	6.36	0.61	131	-	45.53%
	(040) α	16.73	5.29	0.75	107		
	(130) α	18.37	4.82	0.74	109		
16L	(110) α	13.71	6.45	0.61	131	11.46%	46.89%
	(300) β	15.72	5.63	0.55	145		
	(040)α	16.57	5.34	0.79	102		
	(130)α	18.14	4.88	0.69	116		
64L	(110) α	13.94	6.34	0.64	125	10.74%	46.91%
	(300) β	15.98	5.54	0.67	120		
	(040) α	16.82	5.26	0.82	98		
	(130) α	18.38	4.82	0.79	102		
64L after heat treatment	(110) α	13.94	6.34	0.65	123	3.2%	47.12%
	(300) β	15.99	5.54	0.51	159		
	(040) α	16.74	5.29	0.56	143		
	(130) α	18.38	4.82	0.74	109		

To study the crystal structure of HPP, the separation of crystalline peaks from the amorphous halo were made by the fitting of WAXD results through nonlinear software.[31] The degree of crystallinity (X_c) is obtained by:

$$X_c = \frac{A_c}{A_a + A_c} \times 100\% \quad (2)$$

where A_a and A_c are the areas of the amorphous and the total crystal peaks, respectively.

The k value corresponding to the fraction of the β form crystal in the total crystalline phase is calculated from X-ray diffractograms according to Turner–Jones formula[32]:

$$k = \frac{I_{300}}{I_{300} + I_{110} + I_{040} + I_{130}} \quad (3)$$

where I_{300}, I_{110}, I_{040}, and I_{130} are the intensities of [300], [110], [040], and [130] diffractions, respectively. The interplanar spacing (d) and apparent crystal size (L_{hkl}) values for the different peaks can be calculated by Bragg's law and Scherrer's formula,[30] respectively.

$$d = \frac{\lambda}{2 \sin \theta} \quad (4)$$

$$L_{hkl} = \frac{0.9\lambda}{\beta \cos \theta} \quad (5)$$

where λ is the wavelength of radiation used, β is the half-width of the diffraction peaks.

Table I summarizes the crystal structural parameters determined based on WAXD curves. It was clear that the degree of crystallinity (X_c) for different samples showed little change, i.e. X_c would not become a factor causing the discrepancies of plastic deformation for different PP/POE systems. However, the fractions of the β form crystal in the 16-layer and 64-layer samples were a little higher than that in the neat HPP. Our previous researches[33,34] showed that, when polymer melts flowed through a LME, the laminating-multiplying process could induce a strong shearing and elongational force on melts, which could contribute to the formation of β form crystals. In addition, the crystal sizes of $L_{(110)\alpha}$, $L_{(040)\alpha}$, $L_{(130)\alpha}$, and $L_{(300)\beta}$ in the multilayered structure were obviously smaller compared with neat

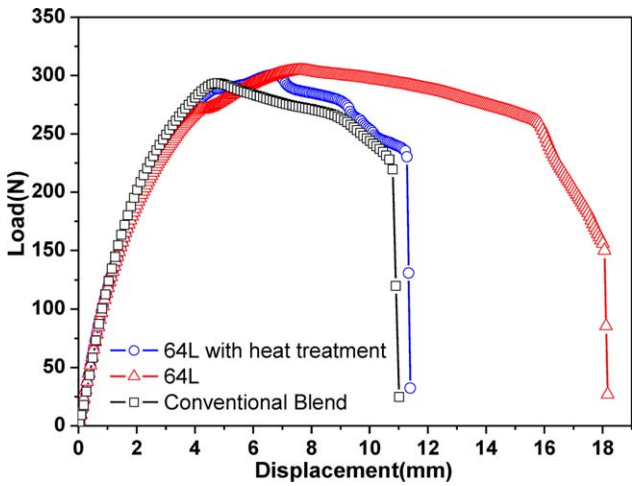

Figure 8. The tear load-displacement curves of 64L, 64L with heat treatment and conventional blend samples. [Color figure can be viewed in the online issue, which is available at wileyonlinelibrary.com.]

HPP and blend sample. And the crystal sizes in the multilayered structure could further decrease with the number of layers increasing. And the unstable β form crystal and smaller crystal size could contribute to the enhanced toughness of polypropylene, causing the large plastic deformation occurring.[35–37]

Mechanism of Ductile Tear Behavior

To prove the effect of crystal structure on the mechanical property of HPP, the 64-layer sample was selected to experience the heat treatment. The original crystal structure produced during the processing would melt at 190 °C for 10 min, and then the molecular chain of HPP recrystallized at a slow cooling rate. Thus, the effect of crystal structure changes on the tear property of 64-layer with heat treatment would be investigated. The tear load-displacement curves of the 64-layer sample with heat treatment, together with 64-layer and conventional blend samples, are shown in Figure 8. It was found that all samples revealed a characteristic of ductile tear fracture behavior. The tear displacement of 64-layer with heat treatment obviously decreased compared with the 64-layer sample that did not experience the heat treatment. The tear strength, which was related to the maximum load during tear testing, did not show any difference. However, both the maximum load and tear displacement of 64-layer sample after heat treatment were still higher than those of conventional blend. The obtained tear results are shown in Figure 9. After heat treatment, the tear strength showed little change, but the tear energy obviously decreased, revealing a lower resistance to tear. The crystal structural parameters of 64-layer sample after heat treatment are summarized in Table I. The fraction of the β form crystal was very low, only 3.2%. And the crystal size clearly increased. Therefore, it can be concluded that the nature of the crystal phase and the crystal size could have an important effect on the plastic deformation behavior during tear. The unstable β form crystal and small crystal size could obviously contribute to the tear toughness.[38]

Although the 64-layer and the blend samples had the similar crystal structures, the tear energy of 64-layer sample was still higher than that of the blend sample. This implied that there were some other factors affecting the plastic deformation of HPP. The optical images of blend, 64-layer and 64-layer with heat treatment samples during tear are shown in Figure 10. The crack propagation scenes were displayed here. For the blend sample, the formed crack could have a large volume and continuously propagate forward, revealing a characteristic of rapid expansion. Therefore, the crack resistance was low, resulting in a small plastic deformation and tear energy. However, for the 64-layer sample, the micro-crack could firstly form in the brittle HPP layer, and then transversely expand to the elastic POE layer. Finally, the micro-cracks were terminated by the interface and could hardly grow into large crack. Therefore, during tear, the cracks in the HPP layer could hardly expand along the thickness direction. And the large plastic deformation of HPP layer would occur before the final fracture. Then the tear energy could be obviously enhanced. After heat treatment, the multilayered structure was not changed, and the interfaces still existed in the multilayered 64-layer sheets. Similarly, during tear, the micro-cracks in the brittle HPP layer could also be hindered by interface. And the rapid crack propagation would be delayed. That was to say, the termination of micro-cracks by interface contributed to the toughness of HPP, resulting in the tear energy of 64-layer with heat treatment sample higher than that of conventional blend sample. Therefore, it could be concluded that the synergistic effect of the crystal structure and the termination of micro-cracks by interface was the fundamental reason that caused the tear resistance of multilayered sheets enhanced.

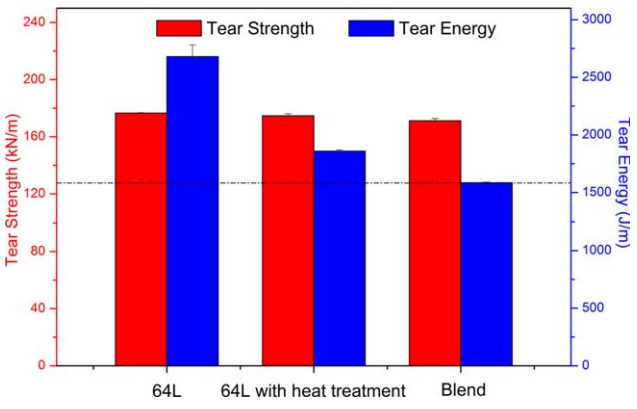

Figure 9. The tear strength and energy of 64L, 64L with heat treatment and bend samples. [Color figure can be viewed in the online issue, which is available at wileyonlinelibrary.com.]

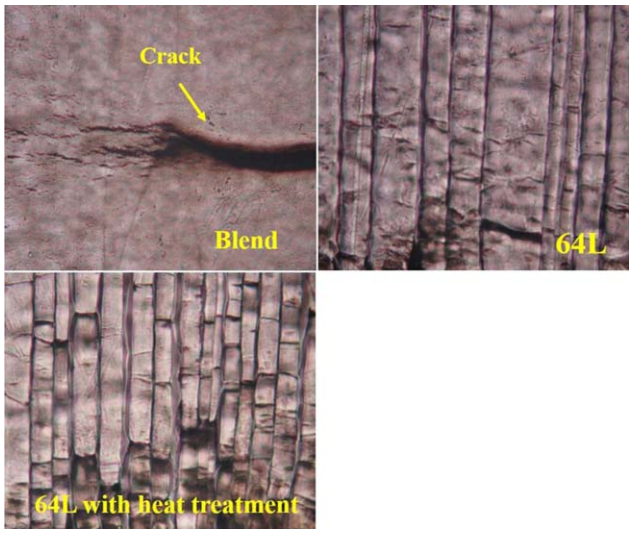

Figure 10. The optical images of blend, 64L and64L with heat treatment samples during tear. [Color figure can be viewed in the online issue, which is available at wileyonlinelibrary.com.]

CONCLUSIONS

In this work, the tear resistance of HPP/POE alternating multilayered sheets was investigated by a Die C type tear test. The results showed that the tear strength of the multilayered sheets was a little higher than that of the conventional blend, and show little change with the number of layers, which correlated with the best phase continuity of multilayered structure in the direction of the acting force. However, the tear energy was

increased with the addition of elastomer POE. During the tear process of multilayer samples, large plastic deformation could accompany the propagation of tear crack, causing the fracture displacement and tear energy obviously increased. The tear energy of multilayered samples was higher than that of conventional blend sample, and could be further enhanced with the number of layers increasing. Through the measurements of 2D-IR and WAXD, it was found that the large plastic deformation of HPP was directly correlated with the crystal structure, including the β form crystal and the decreased crystal size. Besides, the termination of micro-cracks by interface could also improve the tear toughness. Therefore, the high tear resistance of the multilayered sheets was relied on the synergistic effect of the crystal structure and the termination of micro-cracks by interface.

ACKNOWLEDGMENTS

The authors are grateful to the National Natural Science Foundation of China (51227802, 51473103, 51421061, and 51273132), the Sichuan Province Youth Science Fund (2014JQ0001), and the Innovation Team Program of Science & Technology Department of Sichuan Province (Grant 2014TD0002) for financial support of this work.

REFERENCES

1. Kim, H. S.; Karger-Kocsis, J. *Acta Mater.* **2004**, *52*, 3123.
2. Shi, D.; Liu, E.; Tan, T.; Shi, H.; Jiang, T.; Yang, Y.; Luan, S.; Yin, J.; Mai, Y. W.; Li, R. K. Y. *RSC Adv.* **2013**, *3*, 21563.
3. George, S.; Prasannakumari, L.; Koshy, P.; Varughese, K.; Thomas, S. *Mater. Lett.* **1996**, *26*, 51.
4. Veenstra, H.; Verkooijen, P. C. J.; van Lent, B. J. J.; van Dam, J.; de Boer, A. P.; Nijhof, A. P. H. *J. Polym.* **2000**, *41*, 1817.
5. Kolarik, J. *Polym. Eng. Sci.* **1996**, *36*, 2518.
6. Kolark, J. *Eur. Polym. J.* **1998**, *34*, 585.
7. Wang, J.; Wang, C.; Zhang, X.; Wu, H.; Guo, S. *RSC Adv.* **2014**, *4*, 20297.
8. Shen, J.; Wang, M.; Li, J.; Guo, S.; Xu, S.; Zhang, Y.; Li, T.; Wen, M. *Eur. Polym. J.* **2009**, *45*, 3269.
9. Shin, E.; Hiltner, A.; Baer, E. *J. Appl. Polym. Sci.* **1993**, *47*, 269.
10. Haderski, D.; Sung, K.; Im, J.; Hiltner, A.; Baer, E. *J. Appl. Polym. Sci.* **1994**, *52*, 121.
11. Baer, E.; Hiltner, A.; Keith, H. *Science* **1987**, *235*, 1015.
12. He, G.; Zhang, F.; Huang, L.; Li, J.; Guo, S. *J. Appl. Polym. Sci.* **2014**, *131*, 40574.
13. Wu, R. Y.; McCarthy, L. D.; Stachurski, Z. H. *Int. J. Fracture* **1993**, *68*, 141.
14. Kerns, J.; Hsieh, A.; Hiltner, A.; Baer, E. *J. Appl. Polym. Sci.* **2000**, *77*, 1545.
15. He, G.; Li, J.; Zhang, F.; Lei, F.; Guo, S. *Polymer* **2014**, *55*, 1583.
16. Chang, A. C.; Inge, T.; Tau, L.; Hiltner, A.; Baer, E. *Polym. Eng. Sci.* **2002**, *42*, 2202.
17. Chang, A. C.; Tau, L.; Hiltner., A.; Baer, E. *Polymer* **2002**, *43*, 4923.
18. Phulkerd, P.; Hagihara, H.; Nobukawa, S.; Uchiyama, Y.; Yamaguchi, M. *J. Polym. Sci. B: Polym. Phys.* **2013**, *51*, 897.
19. Mollova, A.; Androsch, R.; Mileva, D.; Gahleitner, M.; Funari, S. S. *Eur. Polym. J.* **2013**, *49*, 1057.
20. Zhao, H.; Li, R. K. Y. *Mech. Mater.* **2006**, *38*, 100.
21. Triki, E.; Vu-Khanh, T.; Nguyen-Tri, P.; Boukehili, H. *Theor. Appl. Fract. Mec.* **2012**, *61*, 33.
22. Pan, R.; Wati, D. *Polym. Compos.* **1996**, *17*, 486.
23. Shen, J.; Li, J.; Guo, S. *Polymer* **2012**, *53*, 2519.
24. Zhang, X.; Wu, H.; Guo, S.; Wang, Y. *Polymer* **2013**, *54*, 5429.
25. Zhang, X.; Xie, F.; Pen, Z.; Zhang, Y.; Zhou, W. *Eur. Polym. J.* **2002**, *38*, 1.
26. Tordjeman, P.; Robert, C.; Marin, G.; Gerard, P. *Eur. Phys. J. E.* **2001**, *4*, 459.
27. Chen, Y.; Huang, Z.; Li, Z.; Tang, J.; Hsiao, B. S. *RSC Adv.* **2014**, *4*, 14766.
28. Zheng, K.; Liu, R.; Huang, Y. *Polym. J.* **2010**, *42*, 81.
29. Morita, S.; Shinzawa, H.; Noda, I.; Ozaki, Y. *Appl. Spectrosc.* **2006**, *60*, 398.
30. Ying, J.; Liu, S.; Guo, F.; Zhou, X.; Xie, X. *J. Therm. Anal. Calorim.* **2008**, *91*, 723.
31. Lima, M. F. S.; Vasconcellos, M. A. Z.; Samios, D. *J. Polym. Sci. B Polym. Phys.* **2002**, *40*, 896.
32. Varga, J. *J. Therm. Anal.* **1989**, *35*, 1891.
33. Yang, S.; Yu, H.; Lei, F.; Li, J.; Guo, S.; Wu, H.; Shen, J.; Xiong, Y.; Chen, R. *Macromolecules* **2015**, *48*, 3965.
34. Shen, J.; Wang, M.; Li, J.; Guo, S. *Polym. Adv. Technol.* **2011**, *22*, 237.
35. Shinohara, Y.; Yamazoe, K.; Sakurai, T.; Kimata, S.; Maruyama, T.; Amemiya, Y. *Macromolecules* **2012**, *45*, 1398.
36. Chen, H. B.; Karger-Kocsis, J.; Wu, J. S.; Varga, J. *Polymer* **2002**, *43*, 6505.
37. Nitta, K.; Odaka, K. *Polymer* **2009**, *50*, 4080.
38. Qiu, B.; Chen, F.; Shangguan, Y.; Zhang, L.; Lin, Y.; Zheng, Q. *RSC Adv.* **2014**, *4*, 58999.